Effects of Random Circuit Fabrication Errors on the Mean and Standard Deviation of Small Signal Gain and Phase of a Traveling Wave Tube

Ian M. Rittersdorf, *Student Member, IEEE,* Thomas M. Antonsen, Jr., *Fellow, IEEE,* David Chernin, and Y. Y. Lau, *Fellow, IEEE*

***Abstract*—Random fabrication errors may have detrimental effects on the performance of traveling wave tubes (TWTs) of all types, especially in the sub-millimeter wavelength regime and beyond. Previous studies calculated the standard deviation of the small signal gain and the output phase of a TWT in the presence of small random, axially varying perturbations in the circuit phase velocity, assuming synchronous interaction and zero AC space charge effects. This paper relaxes the latter assumptions. In addition, we calculate the ensemble-average gain and the ensemble-average phase that result from random axial variations in the circuit phase velocity, using two analytic approaches. One is a perturbative approach including all three modes of the coupled beam-circuit equations. The other treats the evolution of only the dominant (exponentially growing) mode. The analytical results on the expected gain and phase compare favorably with results from numerical integrations of the governing equation in the absence of space charge, but are found to deviate from the numerical integrations with the inclusion of space charge effects. The effects of small pitch errors in a 210 GHz folded waveguide TWT are evaluated in an example.**

***Index Terms*—Gain variation, phase variation, traveling wave tube, fabrication tolerance.**

I. Introduction

THE TRAVELING wave tube (TWT) is a key element in telecommunication systems, satellite-based transmitters, military radar, electronic countermeasures, and communication data links [1−4]. Variations in performance due to finite fabrication tolerances in the manufacturing process can lower the fraction of TWTs that meet specifications and drive up the cost of manufacturing [5], [6]. These errors produce proportionately larger perturbations to the circuit as the circuit size is reduced. Their effects on the small signal gain and output phase have been studied by Pengvanich *et. al.* [7] who considered the evolution of the three forward waves in a TWT in which the Pierce parameters vary randomly along the tube axis. A peculiar feature of the results in [7] is that, in the statistical evaluation of a large number of samples with random errors in the circuit phase velocity, a significant number of these samples show an output gain that is higher than the corresponding error-free tube. It is this intriguing feature that prompted us to analyze the expectation values of the gain and phase reported in this paper. As we shall see shortly, we provide an explanation of this statistical feature in this paper. We also extend Ref. [7] to include AC space charge effects and non-synchronous interactions. We shall ignore the effects of the reverse propagating circuit wave, which we recently analyzed [8]. In Ref. [8], we found that reflections may significantly increase the statistical effects on the gain and the output phase. Effects on the TWT backward-wave mode [9] by random manufacturing errors were also recently analyzed [10].

The standard deviations in the gain and in the output phase, which were analytically calculated in Ref. [7], required only an account of the first order effects of random errors. The expected mean of the output gain and phase, which is our focus here, requires consideration of the second order effects of random errors, and is therefore more difficult to evaluate. Since deviation from the mean (a second order effect) is much less than the standard deviation (a first order effect), a significant number of the samples in a statistical analysis would naturally show an output gain that is higher than the corresponding error-free tube, as observed in Pengvanich *et. al.* [7]. We use three approaches to analyze this problem. The first approach is analytical where we apply successive perturbations on all three forward waves. The second approach is also analytical where we include only the dominant, growing mode in the analysis. The third approach is purely numerical where we numerically integrate the governing differential equation (at least) 5000 times using as many random samples in the coefficients that represent random axial variations in the circuit phase velocity. Comparison of these three approaches is presented.

This paper is organized as follows. Section II presents the model to evalute the gain and phase of a traveling wave

Manuscript received January 14, 2013; revised April 5, 2013 and July 10, 2013; accepted July 12, 2013. Date of publication July 17, 2013; date of current version August 26, 2013. This work was supported in part by the Air Force Office of Scientific Research, the Office of Naval Research, and the L-3 Communications Electron Device Division. The review of this paper was arranged by Editor M. Anwar.

I. M. Rittersdorf is with the University of Michigan, Ann Arbor, MI 48108 USA (e-mail: ianrit@umich.edu).

T. M. Antonsen, Jr. is with the University of Maryland, College Park, MD 20742 USA (e-mail: antonsen@glue.umd.edu).

D. Chernin is with Science Applications International Corporation, McLean, VA 22102 USA (e-mail: david.chernin@saic.com).

Y. Y. Lau is with the University of Michigan, Ann Arbor, MI 48108 USA, and also with the Naval Research Laboratory, Washington, DC 20375 USA (e-mail: yylau@umich.edu).

Color versions of one or more of the figures in this paper are available online at http://ieeexplore.ieee.org.

Digital Object Identifier 10.1109/JEDS.2013.2273794

tube for a general ratio of circuit phase velocity to beam velocity, including the effects of space charge. Section III presents the analytic expressions for the expected gain and phase, and for the standard deviations. The details of the two analytical formulations are given in Appendicies A and B. Section IV presents comparison of numerical results from the three different approaches. An example of a 210 GHz, G-band TWT is presented. Section V summarizes our results.

II. Model

We follow the model of Ref. [7] which is based on Pierce's theory except that the assumption of axial uniformity in the circuit parameters has been relaxed. Assuming $e^{j\omega t}$ dependence, the linearized force law, including the "AC space charge effects," reads,

$$\left[\left(\frac{\partial}{\partial z}+j\beta_e\right)^2+\beta_q^2\right]s=a, \tag{1}$$

where s is the electronic displacement caused by the normalized circuit electric field a, $\beta_e=\omega/v_0$, $\beta_q\equiv C\beta_e\sqrt{4QC}$, v_0 is the streaming velocity of the electron beam, C is Pierce's dimensionless gain parameter, and QC is Pierce's space charge parameter. In the absence of AC space charge effects, $QC=0$ and Eq. (1) is identical to Eq. (1) of Ref. [7]. The slow-wave circuit equation is unchanged by the presence of AC space charge,

$$\left(\frac{\partial}{\partial z}+j\beta_p+\beta_e Cd\right)a=-j\left(\beta_e C\right)^3 s, \tag{2}$$

which is the corrected form of Eq. (2) of Ref. [7]. (The third term on the left hand side of Eq. (2) should read $\beta_e Cd$ instead of $\beta_p Cd$, a typo in [7] that has propagated through the literature.) In Eq. (2), $\beta_p=\omega/v_p$, where v_p is the phase velocity of the slow wave in the absence of the beam, and d is the normalized cold tube circuit loss rate. For an error-free tube in which β_p, C, and d are constants, Eqs. (1) and (2) yield the Pierce dispersion relation,

$$\left(\delta^2+4QC\right)\left(\delta+jb+d\right)=-j, \tag{3}$$

assuming $e^{j\omega t-j\beta z}$ dependence, where $\delta=-j(\beta-\beta_e)/C\beta_e$, and $b=(v_0/v_p-1)/C$ is the mismatch between the beam and circuit velocities. When the quantities β_p, C, or d are allowed to vary axially, Eq. (3) is no longer applicable, and we combine Eqs. (1) and (2) to yield,

$$\frac{d^3f(x)}{dx^3}+jC(b-jd)\frac{d^2f(x)}{dx^2}+4QC^3\frac{df(x)}{dx}+jC\left(4QC^3(b-jd)+C^2\right)f(x)=0, \tag{4}$$

where $x=\beta_e z$ is the normalized axial distance, and $f(x)=e^{jx}s(x)$ represents Pierce's three-wave solution to the third order ordinary differential equation (4). In the absence of AC space charge effects, $QC=0$ and Eq. (4) reduces to Eq. (5) of Ref. [7]. We solve Eq. (4) subject to the initial conditions at the TWT input ($x=0$),

$$f(0)=0,\ f'(0)=0,\ f''(0)=1, \tag{5}$$

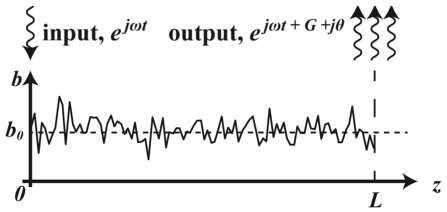

Fig. 1. Sample velocity mismatch profile with a mean value of b_0 of a TWT of length L.

which represent, respectively, zero AC current, zero AC velocity, and unit input electric field. The change in the amplitude gain, G_1 in e-folds, and in the phase, θ_1 in radians, due to random errors is given by,

$$e^{G_1+j\theta_1}=\frac{f''(x)+4QC^3f(x)}{f_0''(x)+4QC^3f_0(x)}, \tag{6}$$

where f_0 represents the solution to Eq. (4) for an error-free tube and the prime denotes differentiation with respect to x. From Eq. (1), we see that Eq. (6) is simply $a(x)/a_0(x)$, where $a_0(x)$ is the error-free solution of $a(x)$.

III. Perturbative and Riccati Approaches

The random manufacturing errors enter the Pierce parameters b, d, and C. It has been shown that the effects of random errors in the velocity parameter, b, dominates those of random errors in d and C [7], so we only consider random errors in b in this paper. Random errors are assigned to $b(x)$ as a set of Gaussian random variables uniformly spaced in x, each with a mean of b_0 and a specified standard deviation, σ_b, as illustrated in Fig. 1. We define the correlation length as $\Delta=L/N$, where N is the number of uniformly spaced nodes over the normalized length (L) of the TWT.

Our work differs from the previous work of Pengvanich *et. al.* by applying the random Gaussian errors directly to the parameter b, instead of to the circuit phase velocity v_p through a dimensionless quantity $q(x)=(v_p(x)-v_{p0})/v_{p0}$, where v_{p0} is the unperturbed circuit phase velocity. The random function $q(x)$ had a specified standard deviation σ_q. The velocity parameter b is related to q by $b(x)=(1/C)[Cb_0-q(x)]/(1+q(x))$ and the standard deviations in b and q are *approximately* related by $\sigma_b=(\sigma_q/C)(1+Cb_0)$. Due to the non-linear relationship between b and q, a Gaussian random error profile assigned to $q(x)$ is no longer Gaussian for $b(x)$. Our numerical integration of Eq. (4) over many 5000-sample calculations shows that this subtle difference led to quantitatively different results. One reason is that the mean deviation is a second order effect in the random error, as we have already mentioned, and this subtle difference is important. In this work, all random errors are characterized by a Gaussian distribution in $b(x)$ with a standard deviation of σ_b.

Pengvanich *et. al.* showed analytically that the standard deviations in the gain and in the output phase from an error-free TWT are first order in σ_b (cf. Eqs. (9a,b) below). In this work, we need to carry out the analysis to second order in the effects of the random errors. With only perturbations in b, we show in Appendix A [cf. Eq. (A16)],

$$\left\langle G_1(x)+j\theta_1(x)\right\rangle = -\frac{1}{2}C^2\sigma_b^2\Delta\left\{\left[4QC^3\sum_{l=1}^{3}\frac{\tau_l}{C\delta_l} + \sum_{k=1}^{3}\tau_k C\delta_k\right]\int_0^x \frac{Q_1(x,s)ds}{a_0(x)} + \sum_{l=1}^{3}\sum_{k=1}^{3} (\tau_l C\delta_l)(\tau_k C\delta_k)\, e^{C(\delta_l+\delta_k)x}\int_0^x \frac{Q_2(x,s)ds}{a_0^2(x)}\right\}, \quad (7)$$

where $\langle G_1(x) + j\theta_1(x)\rangle$ is the ensemble-average deviation in gain and in phase from the error-free tube due to random errors, δ_k (k = 1, 2, 3) are the three roots to the Pierce dispersion relation (3), τ_k (k = 1, 2, 3) which depends only on δ_k, is defined by Eq. (A5) of Ref. [7], and $Q_1(x, s)$, $Q_2(x, s)$ depend only the error-free, three-wave solution. The expressions for $Q_1(x, s)$, $Q_2(x, s)$ are given in Appendix A in Eqs. (A17a,b). Use of Eq. (7) will be referred to as the "perturbation" method.

The second analytical method calculates $\langle G_1(x) + j\theta_1(x)\rangle$ using a Riccati formulation of the complex wave number for a single wave. This formulation yields, [see Appendix B, Eq. (B33)],

$$\langle G_1(x) + j\theta_1(x)\rangle = -\frac{\lambda}{2}\left(\frac{C}{1+Cb_0}\right)^2\sigma_b^2 x\Delta, \quad (8)$$

where λ is a complex value that is determined by the value of the mismatch parameter, b_0. This method will be referred to as the "Riccati" method.

Finally, we revise the standard deviation of gain and phase variations calculated in Ref. [7] to include the space charge effects ($QC \neq 0$). In terms of the standard deviation of b, σ_b, the standard deviation in the gain G_1 and in the phase θ_1 is given by, respectively,

$$\sigma_{Gb} = S_{Gb}\sigma_b, \quad S_{Gb} = \sqrt{\frac{x}{N}}\sqrt{\int_0^x ds\left|g_{br}(x,s)\right|^2} \quad (9a)$$

and

$$\sigma_{\theta b} = S_{\theta b}\sigma_b, \quad S_{\theta b} = \sqrt{\frac{x}{N}}\sqrt{\int_0^x ds\left|g_{bi}(x,s)\right|^2}, \quad (9b)$$

where g_{br} and g_{bi} are the real and imaginary parts, respectively, of g_b, given by

$$g_b(x,s) = -jC\left(4QC^3 f_0(s) + a_0(s)\right)a_0(x-s)/a_0(x). \quad (10)$$

In the absence of space charge, *i.e.* $QC = 0$, Eq. (10) reduces to Eq. (A15) of Ref. [7], whose Eq. (A4) defines the error-free solutions f_0 and a_0.

Equations (9a) and (9b) show that the standard deviations in the gain and phase are linear in σ_b. Equations (7) and (8) show that $\langle G_1(x)\rangle$ and $\langle \theta_1(x)\rangle$ are both quadratic in σ_b, and their magnitudes are therefore much less than the standard deviations. This contrast between the standard deviation, and the deviation in the mean from the error-free tubes, was also apparent in Fig. 8 of Ref. [8].

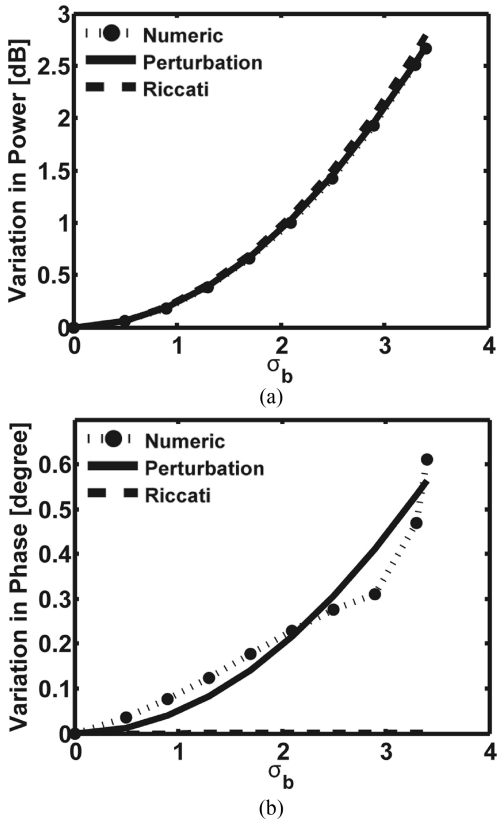

Fig. 2. (a) Mean values of the power and (b) phase at the output relative to the unperturbed values at the output for a synchronous beam velocity, $b_0 = 0$. The points are the results of numerically integrating Eq. (4). The solid and dashed lines show the perturbation and Riccati formulas, Eqs. (7) and (8), respectively. Here, $x = 100$, $C = 0.05$, $\Delta = 1$, $d = 0$, and $QC = 0$.

IV. Results

We start with the TWT base case with length x = 100 where $b_0 = d = QC = 0$, and C = 0.05. Equation (4) yields an error-free gain of 28.1 dB and an output phase of -5872°. Random errors are then introduced into the velocity parameter, b, as shown in Fig. 1. The value at each node is an independent Gaussian random variable with a mean of b_0 and a specified standard deviation, σ_b. A correlation length of Δ = 1 has been used in all calculations, meaning that each node of the Gaussian random error profile would correspond to x = 1, 2, ... , 100 in the TWT. For a specified value of σ_b, we integrate Eq. (4) numerically 5000 times. Previous work [7] showed that performing only 500 integrations would provide sufficient results. That work, however, was focused on calculating the standard deviation in gain and phase and not the mean. While 500 integrations is sufficient to calculate these standard deviations, significantly more are required to calculate the mean accurately, since the mean is second order in σ_b. We have checked that integrating Eq. (4) up to 25,000 times does not provide a significantly different answer, even for phase variations as small as a fraction of a degree given

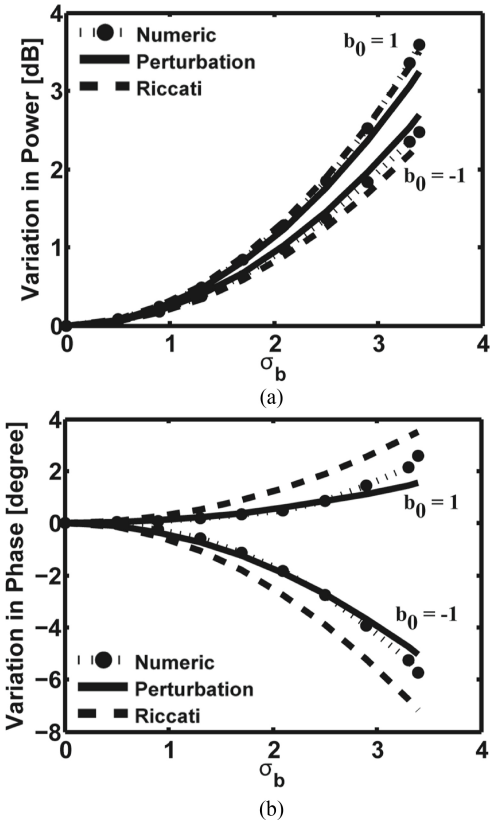

Fig. 3. (a) Mean values of the power and (b) phase at the output relative to the unperturbed values at the output for non-synchronous beam velocities of $\pm 0.05 v_p$ ($b_0 = \pm 1$). The points are the results of numerically integrating Eq. (4). The solid and dashed lines show the perturbation and Riccati formulas, Eqs. (7) and (8), respectively. Here, $x = 100, C = 0.05, \Delta = 1, d = 0$, and $QC = 0$.

in Figs. 2(b) and 7(c). Calculations performed in this manner will be designated as "numerical". One important note is that this numerical calculation is strongly dependent on the random number seed used in these calculations. Different seed values do not produce a difference in the mean gain output, however, the exact values for the output phase will be different albeit of the same order. In all of the following calculations, the seed used for the random number sequence has been fixed.

Figure 2(a) shows the gain variations for the numerical, perturbation, and Riccati methods. All three methods show good agreement. The phase calculation is shown in Fig. 2(b). The perturbation method shows good agreement with the numerical results. It should be noted that in this case $\langle \theta_1(x) \rangle = 0$ for the Riccati method (cf. the last sentence in Appendix B). This result is consistent with those from the perturbative analysis and the numerical solution to Eq. (4), in that the phase variations $\langle \theta_1(x) \rangle$ due to random errors, measured in radians, is found to be negligible compared with the amplitude variations $\langle G_1(x) \rangle$, measured in e-folds, in this case. This case is identical to the one considered by Ref. [7].

Figure 3 shows two cases where the the velocity mismatch is nonzero. For $C = 0.05$, $b_0 = \pm 1$ corresponds to a difference of $\pm 5\%$ between the beam velocity and circuit phase velocity. All three methods are in agreement even when the velocity mismatch is allowed to be nonzero. Looking at the phase

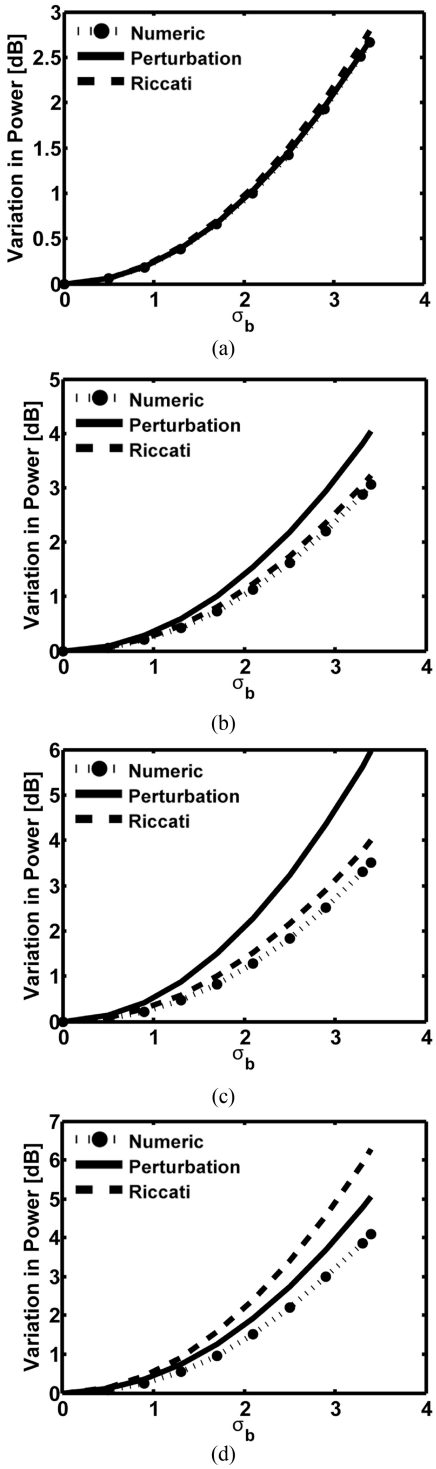

Fig. 4. (a) Mean values of the power at the output relative to the unperturbed values for $QC = 0$, (b) $QC = 0.15$, (c) $QC = 0.25$, and (d) $QC = 0.35$ for the synchronous velocity case, $b_0 = 0$. The points are the results of numerically integrating Eq. (4). The solid and dashed lines show the perturbation and Riccati formulas, Eqs. (7) and (8), respectively. Here, $x = 100$, $C = 0.05$, $\Delta = 1$, and $d = 0$.

output it appears that the perturbation method is more accurate than the Riccati method.

Figures 4 and 5 show how the gain and phase are affected by the inclusion of the QC term, increasing it from 0 to 0.35 for the synchronous case, $b_0 = 0$. When $QC \neq 0$, both the perturbation and Riccati methods predict a larger variation in

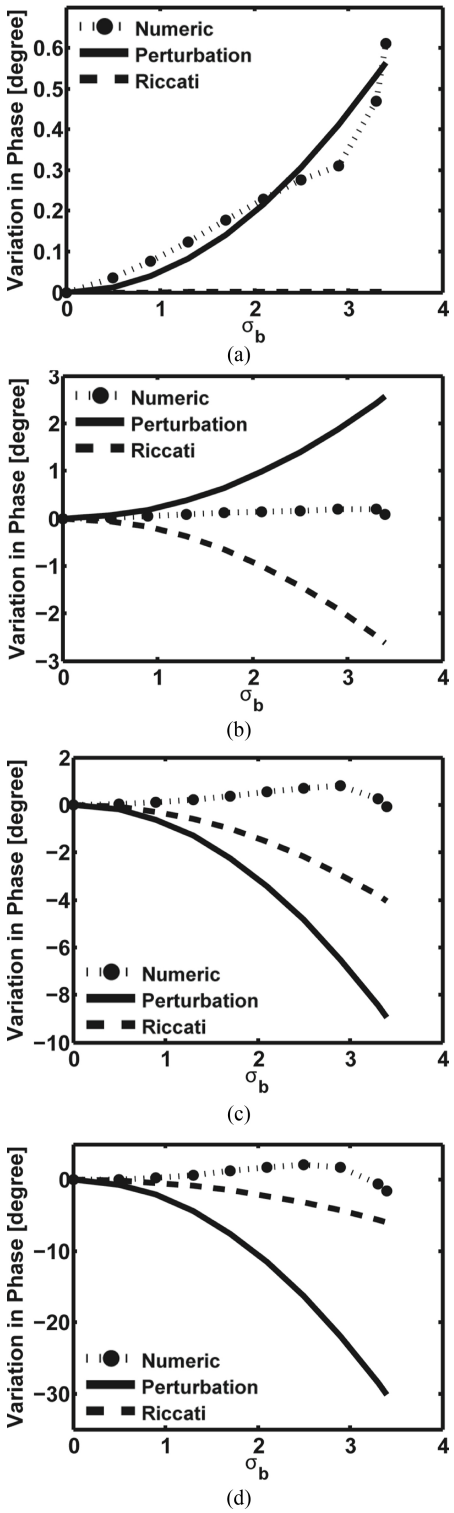

Fig. 5. (a) Mean values of the phase at the output relative to the unperturbed values for $QC = 0$, (b) $QC = 0.15$, (c) $QC = 0.25$, and (d) $QC = 0.35$ for the synchronous velocity case, $b_0 = 0$. The points are the results of numerically integrating Eq. (4). The solid and dashed lines show the perturbation and Riccati formulas, Eqs. (7) and (8), respectively. Here, $x = 100$, $C = 0.05$, $\Delta = 1$, and $d = 0$.

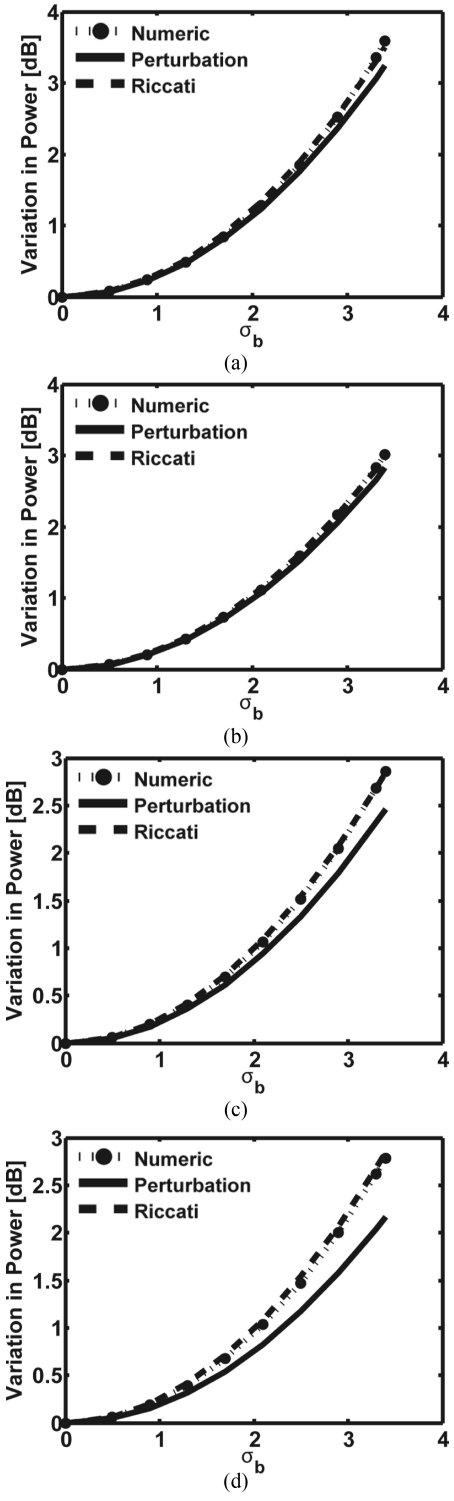

Fig. 6. (a) Mean values of the power at the output relative to the unperturbed values for $QC = 0$, (b) $QC = 0.15$, (c) $QC = 0.25$, and (d) $QC = 0.35$ for the non-synchronous velocity case, $b_0 = 1$. The points are the results of numerically integrating Eq. (4). The solid and dashed lines show the perturbation and Riccati formulas, Eqs. (7) and (8), respectively. Here, $x = 100$, $C = 0.05$, $\Delta = 1$, and $d = 0$.

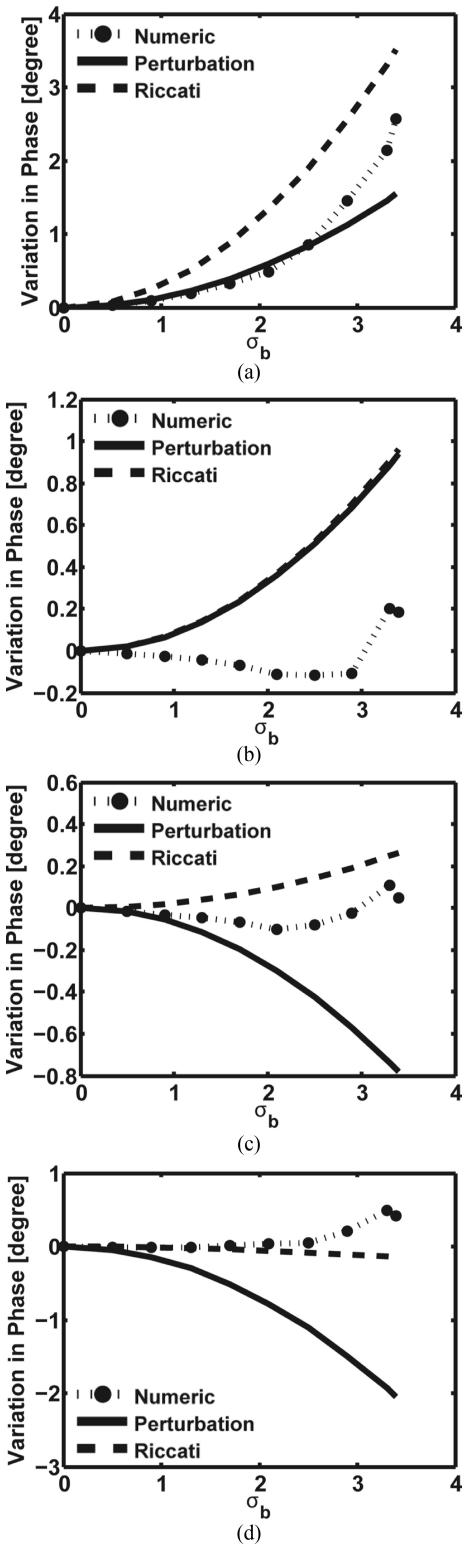

Fig. 7. (a) Mean values of the phase at the output relative to the unperturbed values for $QC = 0$, (b) $QC = 0.15$, (c) $QC = 0.25$, and (d) $QC = 0.35$ for the non-synchronous velocity case, $b_0 = 1$. The points are the results of numerically integrating Eq. (4). The solid and dashed lines show the perturbation and Riccati formulas, Eqs. (7) and (8), respectively. Here, $x = 100$, $C = 0.05$, $\Delta = 1$, and $d = 0$.

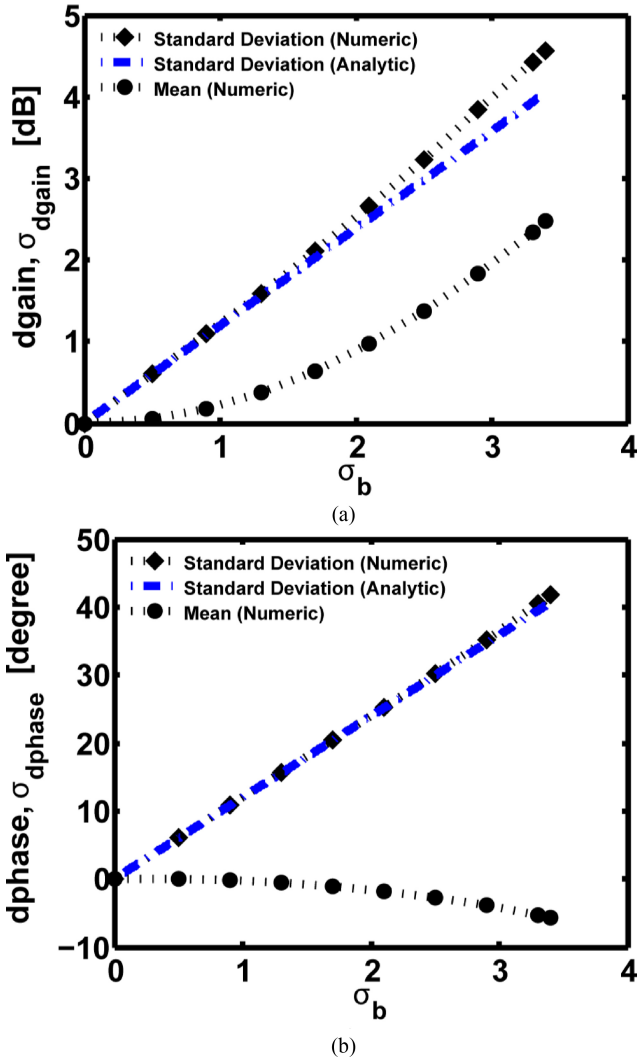

Fig. 8. Mean values and standard deviation of the (a) gain and (b) phase at the output relative to the unperturbed values for $QC = 0$ for the non-synchronous velocity case, $b_0 = -1$. The circles are the results of numerically integrating Eq. (4). The diamonds are the standard deviation results from numerically integrating Eq. (4). The dashed line is the analytic standard deviation as calculated from Eq. (9). Here, $x = 100$, $C = 0.05$, $\Delta = 1$, and $d = 0$.

gain and phase than shown by the numerical analysis. The Riccati method tends to predict smaller variations than the perturbation method, but neither prediction shows agreement with the numerical data. Figures 6 and 7 show the gain and phase variations for QC again increasing from 0 to 0.35, this time for the $b_0 = 1$ case. In this case, the Riccati method shows good agreement with the numerical data for gain. Neither analytical method shows agreement with the numerical phase data in this case. The $b_0 = -1$ case could not be calculated reliably because the TWT would not amplify for any significant values of QC.

Figure 8 shows how the analytical standard deviation calculation from Eq. (9) compares to the statistical standard deviation as calculated from the numerical integration of Eq. (4) for a non-synchronous beam velocity. Both calculations are in agreement over a range of non-synchronous beam velocities. Figure 9 shows the analytical standard deviation as calculated

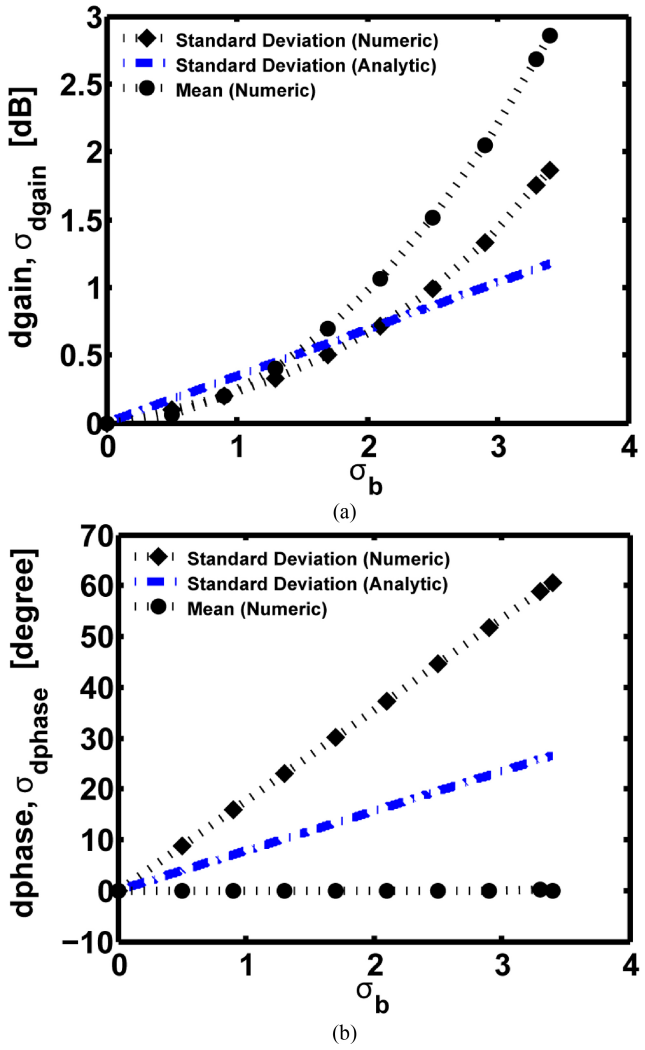

Fig. 9. Mean values and standard deviation of the (a) gain and (b) phase at the output relative to the unperturbed values for $QC = 0.25$ for the non-synchronous velocity case, $b_0 = 1$. The circles are the results of numerically integrating Eq. (4). The diamonds are the standard deviation results from numerically integrating Eq. (4). The dashed line is the analytic standard deviation as calculated from Eq. (9). Here, $x = 100$, $C = 0.05$, $\Delta = 1$, and $d = 0$.

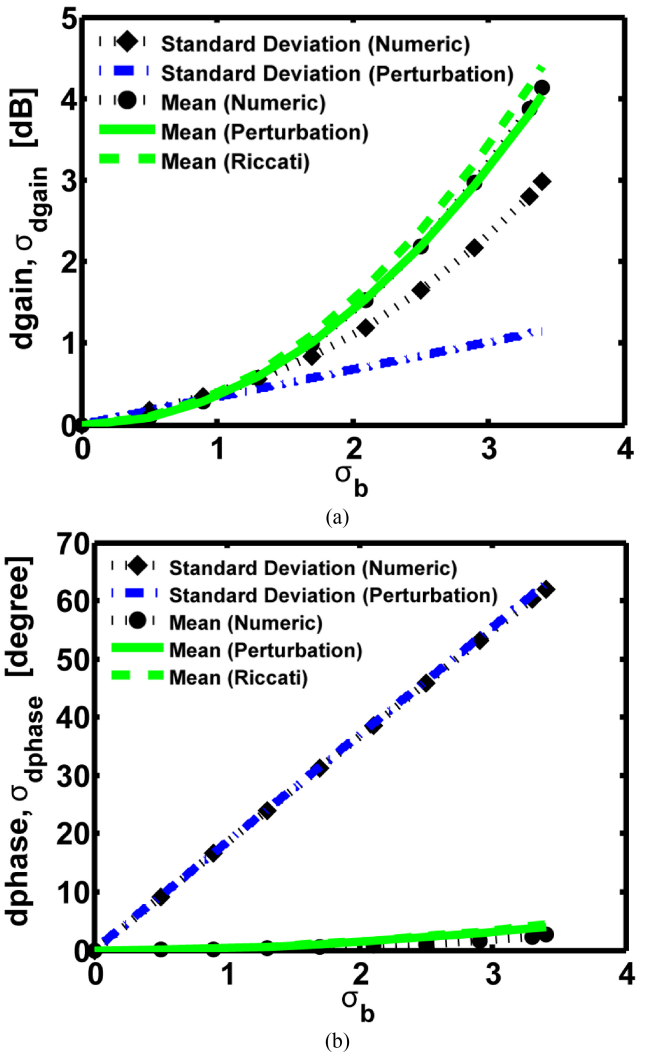

Fig. 10. Mean values and standard deviation of the (a) gain and (b) phase at the output relative to the unperturbed values for a G-band-like TWT. Results from the statistical, perturbation, and Riccati calculations for mean as well as analytic and statistical results for standard deviation are plotted. Here, $x = 240$, $\Delta = 4$, $C = 0.0197$, $b_0 = 0.36$, and $QC = d = 0$.

by Eq. (9) with the space charge modified expression for g_b from Eq. (10), as well as the statistical standard deviation calculation. With the inclusion of the space charge term, QC, Eq. (9) is no longer in agreement with the statistical calculation. The difference between the two increases with increasing values of QC.

Finally, as a concrete example, we consider the G-band (210 GHz) folded waveguide TWT previously studied [8] with a beam voltage of 11.7 kV, a beam current of 120 mA, a length of 1.2 cm, and an average circuit pitch of 0.02 cm. This corresponds to a normalized length of $x = 240$, and we take a correlation length of $\Delta = 4$. For this example we consider the specific case with $C = 0.0197$, $QC = 0$, and $b_0 = 0.36$, using Figs. 11 and 12 of Ref. [8]. Figure 10 shows both the gain and phase variation of this G-Band-like TWT accurately predicted by both the perturbation and Riccati methods. The statistical standard deviations in gain and phase and analytic formula are also presented in Figure 10, showing good agreement as well. Results for the standard deviation using the Riccati approach are not yet available.

V. Summary and Conclusion

Two different formulas were derived to predict the deviations in gain and phase in a traveling wave tube in the presence of random axial errors: a second-order perturbation analysis that accounts for all three forward propagating waves and a Riccati analysis that includes only the amplifying wave. We have compared both of these models against a numerical integration of the governing, third-order linear differential equation for cases with nonzero b and the inclusion of AC space charge effects. We have found that the perturbation analytic model shows good agreement with the numerical analysis for non-synchronous beam velocity, *i.e.* nonzero b, in the absence of space charge. We have also found that the analytic models do not accurately predict the TWT behavior

in the presence of AC space charge. A possible explanation is that a nonzero QC would enlarge the range of b in which the amplifying wave would have a reduced or even zero gain, in which case all three waves would have comparable amplitudes.

Since we have shown in this paper that the standard deviation is much larger than the deviation in the mean from an error-free tube, we have essentially solved the puzzle as to why random variations in $b(x)$, presumably caused by manufacturing errors, could lead to a higher gain in a significant fraction of the samples simulated [7]. Identification of the types of random errors that would lead to higher gain awaits further study.

Appendix A
Second-Order Small-Signal Solution in the Presence of Random Errors

We derive the second-order perturbative solution to Eq. (4) when the Pierce parameters C and d are constant and the parameter b contains small random perturbations denoted as $b_1(x)$. We re-write Eq. (6) as,

$$a = a_0 e^{G_1 + j\theta_1}, \tag{A1}$$

where a is the normalized electric field and $a_0(x)$ is the solution in the error-free tube given by Eq. (A4) of [7]. To second order, we write $a(x) = a_0(x) + a_{10}(x) + a_{11}(x)$. The first and second order perturbations are $a_{10}(x)$ and $a_{11}(x)$, respectively. Expanding $a(x)$ in Eq. (A1) yields an expression for the modification of amplitude and phase of

$$G_1 + j\theta_1 = \frac{a_{10} + a_{11}}{a_0} - \frac{1}{2}\frac{a_{10}^2}{a_0^2}. \tag{A2}$$

This equation can be solved for the gain and phase change when the expressions for a_{10} and a_{11} are substituted into Eq. (A2). These quantities are to be derived in this appendix.

Equation (4) can be written as three coupled first-order differential equations expressed in matrix notation as

$$\frac{d\mathbf{Y}}{dx} = (\mathbf{M} + \mathbf{M}_1)\,\mathbf{Y}, \tag{A3}$$

in the presence of random variation $b_1(x)$, where

$$\mathbf{M} = \begin{bmatrix} 0 & 1 & 0 \\ 0 & 0 & 1 \\ -jC\left(4QC^3(b-jd)+C^2\right) & -4QC^3 & -jC(b-jd) \end{bmatrix}, \tag{A4}$$

$$\mathbf{M}_1 = \begin{bmatrix} 0 & 0 & 0 \\ 0 & 0 & 0 \\ m_{31}(x) & 0 & m_{33}(x) \end{bmatrix}, \tag{A5}$$

where $m_{31}(x) = -jC\left(4QC^3\right) b_1(x)$ and $m_{33}(x) = -jCb_1(x)$. Equation (A4) is a constant matrix containing error-free tube parameters. Equation (A5) is a matrix containing the random perturbations. We assume that there are no losses, *i.e.* $d = 0$. We write

$$\mathbf{Y} = \mathbf{Y}_0(x) + \mathbf{Y}_1(x) \equiv \begin{bmatrix} f_0(x) + f_1(x) \\ v_0(x) + v_1(x) \\ a_0(x) + a_1(x) \end{bmatrix}, \tag{A6}$$

where quantities with subscript 1 are due only to random $b_1(x)$. The error-free solutions are f_0, v_0, and a_0 and are given by Eq. (A4) of [7]. Combining Eq. (A6) with (A3) yields, to second order

$$\frac{d\mathbf{Y}_1(x)}{dx} - \mathbf{M}\mathbf{Y}_1(x) = \mathbf{M}_1\mathbf{Y}_0(x) + \mathbf{M}_1\mathbf{Y}_1(x). \tag{A7}$$

Ignoring the second order term $\mathbf{M}_1\mathbf{Y}_1(x)$, the solution to Eq. (A7) is $\mathbf{Y}_1(x) = \mathbf{Y}_{10}(x)$, whose solution is given by Eq. (A10) of [7]. Next, let us approximate $\mathbf{M}_1\mathbf{Y}_1(x)$ in Eq. (A7) as $\mathbf{M}_1\mathbf{Y}_{10}(x)$, and write

$$\mathbf{Y}_1 = \mathbf{Y}_{10}(x) + \mathbf{Y}_{11}(x) \equiv \begin{bmatrix} f_{10}(x) + f_{11}(x) \\ v_{10}(x) + v_{11}(x) \\ a_{10}(x) + a_{11}(x) \end{bmatrix}. \tag{A8}$$

Equation (A7) then becomes

$$\frac{d\mathbf{Y}_{11}(x)}{dx} - \mathbf{M}\mathbf{Y}_{11}(x) \cong \mathbf{M}_1(x)\mathbf{Y}_{10}(x), \tag{A9}$$

which is of the same form as Eq. (A7) of [7]. We may then express $\mathbf{Y}_{11}(x)$ as Eq. (A10) from [7] to obtain

$$a_{11}(x) = \int_0^x ds\,\left(m_{31}(s) f_{10}(s) + m_{33}(s) a_{10}(s)\right) P_3(x, s), \tag{A10}$$

where

$$P_3(x, s) = \Psi_{31}(x)\Psi_{13}^{-1}(s) + \Psi_{32}(x)\Psi_{23}^{-1}(s) + \Psi_{33}(x)\Psi_{33}^{-1}(s), \tag{A11}$$

and $\Psi_{ij}(x)$ $(i, j = 1, 2, 3)$ is defined by Eq. (A3) of [7]. The first order perturbations $f_{10}(x)$ and $a_{10}(x)$ are given by Eq. (A11) of [7], where the expression for $V_k(s)$ now contains the AC space charge term in $m_{31}(x)$. Substituting these into Eq. (A10) yields

$$\begin{aligned} a_{11}(x) = \int_0^x ds\, P_3(x, s) \Bigg\{ & \sum_{l=1}^{3} \frac{\tau_l}{C\delta_l} e^{C\delta_l s} \int_0^s ds'\, e^{-C\delta_l s'} \\ & \times \left[f_0(s') m_{31}(s') m_{31}(s) + a_0(s') m_{33}(s') m_{31}(s) \right] \\ & + \sum_{k=1}^{3} \tau_k C\delta_k e^{C\delta_k s} \int_0^s ds'\, e^{-C\delta_k s'} \\ & \times \left[f_0(s') m_{31}(s') m_{33}(s) + a_0(s') m_{33}(s') m_{33}(s) \right] \Bigg\}, \end{aligned} \tag{A12}$$

where δ_k $(k = 1, 2, 3)$ are the three roots to the Pierce dispersion relation (3), and τ_k $(k = 1, 2, 3)$ which depends only on δ_k, is defined by Eq. (A5) of Ref. [7].

We next take the ensemble-average of Eq. (A12), assuming that $\langle b_1(s) b_1(s') \rangle = \langle b_1^2 \rangle\, \Delta\delta(s - s')$, where Δ is the correlation length and δ is the Dirac delta function. With $\langle b_1^2 \rangle = \sigma_b^2$, we obtain

$$\langle a_{11}(x)\rangle = -C^2\sigma_b^2\Delta\int_0^x ds\, P_3(x,s) \times\left\{\left(4QC^3\right)\sum_{l=1}^{3}\frac{\tau_l}{C\delta_l}\left[4QC^3\frac{f_0(s)}{2}+\frac{a_0(s)}{2}\right] +\sum_{k=1}^{3}\tau_k C\delta_k\left[4QC^3\frac{f_0(s)}{2}+\frac{a_0(s)}{2}\right]\right\}. \quad \text{(A13)}$$

Similarly, squaring $a_{10}(x)$ and taking the ensemble-average yields

$$\left\langle a_{10}^2(x)\right\rangle = -C^2\sigma_b^2\Delta\sum_{k=1}^{3}\sum_{l=1}^{3}(\tau_k C\delta_k)(\tau_l C\delta_l)\,e^{C(\delta_k+\delta_l)x} \times\int_0^x ds\, e^{-C(\delta_k+\delta_l)s}\left[\left(4QC^3\right)^2 f_0^2(s) +2\left(4QC^3\right) f_0(s)a_0(s)+a_0^2(s)\right]. \quad \text{(A14)}$$

Note that $\langle a_{10}(x)\rangle = 0$ since $\mathbf{M}_1$ is linear in $b_1(x)$ and therefore $\langle \mathbf{Y}_{10}(x)\rangle = 0$ (cf. Eq. (A10) of [7]). With this result, we obtain from Eq. (A2),

$$\langle G_1(x)+j\theta_1(x)\rangle = \frac{\langle a_{11}(x)\rangle}{a_0(x)} - \frac{1}{2}\frac{\left\langle a_{10}^2(x)\right\rangle}{a_0^2(x)}, \quad \text{(A15)}$$

where $\langle a_{11}(x)\rangle$ is given by Eq. (A13), $a_0(x)$ by Eq. (A4) of [7], and $\left\langle a_{10}^2(x)\right\rangle$ by Eq. (A14). This can be written in the form

$$\left\langle G_1(x)+j\theta_1(x)\right\rangle = -\frac{1}{2}C^2\sigma_b^2\Delta\left\{\left[4QC^3\sum_{l=1}^{3}\frac{\tau_l}{C\delta_l}+ \sum_{k=1}^{3}\tau_k C\delta_k\right]\int_0^x\frac{Q_1(x,s)ds}{a_0(x)}+\sum_{l=1}^{3}\sum_{k=1}^{3}(\tau_l C\delta_l) (\tau_k C\delta_k)\,e^{C(\delta_l+\delta_k)x}\int_0^x\frac{Q_2(x,s)ds}{a_0^2(x)}\right\}, \quad \text{(A16)}$$

which is Eq. (7) of the text. In Eq. (A16), $Q_1(x,s)$, $Q_2(x,s)$ are given by, with the substitution $\lambda_i = C\delta_i$,

$$Q_1(x,s) = \left\{\left[\lambda_1^2(\lambda_2-\lambda_3)\,e^{\lambda_1(x-s)}+\lambda_2^2(\lambda_1-\lambda_3)\,e^{\lambda_2(x-s)} +\lambda_3^2(\lambda_1-\lambda_2)\,e^{\lambda_3(x-s)}\right]\left[\sum_{i=1}^{3}\lambda_i\tau_i e^{\lambda_i s}+4QC^3 \times\sum_{j=1}^{3}\frac{\tau_j}{\lambda_j}e^{\lambda_j s}\right]\right\}\Big/\left[(\lambda_1-\lambda_2)(\lambda_1-\lambda_3)(\lambda_2-\lambda_3)\right], \quad \text{(A17a)}$$

$$Q_2(x,s) = \left(\frac{1}{\lambda_1\lambda_2\lambda_3}\right)^2 e^{-(\lambda_k+\lambda_l)} \times\left[\tau_1\lambda_2\lambda_3\left(4QC^3+\lambda_1^2\right)e^{\lambda_1 s}+\tau_2\lambda_1\lambda_3\left(4QC^3+\lambda_2^2\right)e^{\lambda_2 s} +\tau_3\lambda_1\lambda_2\left(4QC^3+\lambda_3^2\right)e^{\lambda_3 s}\right]. \quad \text{(A17b)}$$

In the limit of zero space charge effects, Eq. (A16) reduces to

$$\langle G_1(x)+j\theta_1(x)\rangle = -\frac{1}{2}C^2\sigma_b^2\Delta\int_0^x ds\, A(x,s), \quad \text{(A18)}$$

where

$$A(x,s) = \sum_{j=1}^{3}\tau_j C\delta_j P_3(x,s)\frac{a_0(s)}{a_0(x)}+\sum_{k=1}^{3}\sum_{l=1}^{3}(\tau_k C\delta_k)(\tau_l C\delta_l) \times e^{C(\delta_k+\delta_l)x}e^{-C(\delta_k+\delta_l)s}\frac{a_0^2(s)}{a_0^2(x)}. \quad \text{(A19)}$$

Appendix B
Riccati Formulation of Wavenumber for Single Wave

To study the effect on the small-signal gain and phase in a TWT due to small random errors, we begin with the following equations,

$$\left[\left(\frac{d}{dz}-i\frac{\omega}{v_z}\right)^2+k_p^2\right]n = a, \quad \text{(B1)}$$

$$\left[\frac{d^2}{dz^2}+k_s^2(z)\right]a(z) = -2k_0k_g^3n(z), \quad \text{(B2)}$$

where $a(z)$ represents the field amplitude, $n(z)$ represents the perturbed beam density, and we have assumed $e^{-i\omega t}$ dependence for these quantities. The coefficients in (B1) and (B2) represent the following: $k_s(z)$ is the axially varying wave number for the structure. The beam plasma wavenumber is k_p. The nominal gain rate is $k_g = Ck_0$, where C is the Pierce parameter. The unperturbed beam velocity is v_z. It is assumed that $k_s(z)$ is close to some reference value such that,

$$k_s^2(z) = k_0^2+\delta k^2(z), \quad \text{(B3)}$$

where k_0 is defined such that the expectation of the deviation vanishes, $\left\langle \delta k^2(z)\right\rangle = 0$. Equations (B1) and (B2) are equivalent to Eqs. (1) and (2) of the main text if we ignore the reverse propagating mode in Eq. (B2), change the sign of ω, and set $n = s$, $\omega/v_z = \beta_e$, $k_s^2 = \beta_p^2$, $k_p^2 = \beta_q^2$, $k_0 = \beta_{p0}$ (= error-free value), $k_g = Ck_0$, and $i = j = \sqrt{-1}$.

Equation (B2) describes both the forward and backward structure wave. In the presence of random variations in wavenumber there will be a coupling of the forward and backward waves. This is the same coupling that gives rise to Anderson localization in condensed matter physics. If the forward wave is growing in z, the lowest order effect of the conversion of forward wave power into backward wave power is to create an effective attenuation of the forward wave. In other words, we can neglect the conversion of backward wave power back into forward wave power, and assume that the backward wave power is effectively lost. We will not calculate this effect here, except to assume that if we wish, we can add an attenuation to the forward wave at the end of the calculation.

The next step is to write the field amplitude as a sum of forward and backward waves,

$$a(z) = a_+(z)e^{ik_0 z} + a_-(z)e^{-ik_0 z}, \tag{B4}$$

where we choose

$$0 = a'_+(z)e^{ik_0 z} + a'_-(z)e^{-ik_0 z}, \tag{B5}$$

and the prime denotes differentiation with respect to z. We insert (B4) into (B2), use our constraint (B5), drop the backward wave, and introduce the revised density perturbation, $\hat{n} = ne^{-ik_0 z}$, to obtain the third order system describing the coupled forward wave and beam space charge waves,

$$2ik_0 \frac{da_+}{dz} = -\delta k^2(z)a_+ - 2k_0 k_g^3 \hat{n} \tag{B6}$$

$$\left[\left(\frac{d}{dz} + i\Delta k\right)^2 + k_p^2\right]\hat{n} = a_+, \tag{B7}$$

where $\Delta k = k_0 - \omega/v_z$ is the mismatch wavenumber between the structure mode and the beam mode.

We expect the solutions of (B6) and (B7) to correspond on average to exponentially growing waves. The average spatial growth rate will be affected (reduced) by the random variations in structure wavenumber. To calculate this effect we will recast (B6) and (B7) as a nonlinear system of equations for the complex rate of exponentiation of the relevant quantities. Specifically we introduce

$$\mu_+(z) = \frac{1}{a_+}\frac{da_+}{dz}, \tag{B8}$$

and

$$\mu_n(z) = \frac{1}{\hat{n}}\frac{d\hat{n}}{dz}, \tag{B9}$$

and rewrite (B6) and (B7)

$$2ik_0\mu_+ = -\delta k^2(z) - 2k_0 k_g^3 \rho(z) \tag{B10}$$

$$\left[(\mu_n + i\Delta k)^2 + k_p^2\right] + \frac{d}{dz}\mu_n = \rho^{-1}. \tag{B11}$$

Here the quantity $\rho(z) = \hat{n}/a_+$ gives the spatially varying ratio of density perturbation to field amplitude. It satisfies a differential equation,

$$\frac{1}{\rho}\frac{d\rho}{dz} = \mu_n - \mu_+. \tag{B12}$$

It is important to point out that Eqs. (B10)-(B12) are equivalent to (B6) and (B7). That is, the only approximation we have made is to drop the backward structure wave.

We now separate the dynamical variables into mean and fluctuating parts; specifically $\mu_+ = \bar{\mu}_+ + \delta\mu_+$, $\mu_n = \bar{\mu}_n + \delta\mu_n$, and $\rho = \bar{\rho} + \delta\rho$, where the overbar denotes the ensemble mean, which is the same mean that we have previously denoted with angular brackets. We then take the mean of (B10)-(B12),

$$2ik_0\bar{\mu}_+ = -2k_0 k_g^3 \langle\rho\rangle, \tag{B13}$$

$$\left[(\bar{\mu}_n + i\Delta k)^2 + \left\langle(\delta\mu_n)^2\right\rangle + k_p^2\right] = \left\langle\rho^{-1}\right\rangle, \tag{B14}$$

and

$$\left\langle\frac{1}{\rho}\frac{d\rho}{dz}\right\rangle = \frac{d}{dz}\langle\ln\rho\rangle = \bar{\mu}_n - \bar{\mu}_+ = 0. \tag{B15}$$

Thus, from (B15) we see that the field amplitude and density perturbation must grow on average at the same rate, $\bar{\mu}_n = \bar{\mu}_+ \equiv \bar{\mu}$. Evaluation of $\left\langle\rho^{\pm 1}\right\rangle$ in (B13) and (B14) requires integration of Eq. (B12). Specifically, we write $\rho = \rho_0 \exp[\delta\Gamma(z)]$ where ρ_0 is a constant to be determined, and

$$\frac{d}{dz}\delta\Gamma(z) = \delta\mu_n - \delta\mu_+. \tag{B16}$$

We then expand ρ and its inverse under the assumption of small fluctuations in $\delta\Gamma$,

$$\rho^{\pm 1} = \rho_0^{\pm 1}\left(1 \pm \delta\Gamma + \frac{1}{2}\delta\Gamma^2 + ...\right). \tag{B17}$$

We will terminate the series after the third term. We thus have,

$$\left\langle\rho^{\pm 1}\right\rangle = \rho_0^{\pm 1}\left(1 + \frac{1}{2}\left\langle\delta\Gamma^2\right\rangle\right). \tag{B18}$$

We now insert (B18) in (B13) and (B14) and take the product to eliminate ρ_0, giving us a dispersion relation for the common mean rate of change of the exponent, $\bar{\mu}$,

$$D(\bar{\mu}) = D_b(\bar{\mu}) + D_g(\bar{\mu}) = -\left\langle\delta\mu_n^2\right\rangle - D_g\left\langle\delta\Gamma^2\right\rangle, \tag{B19}$$

where $D_b(\bar{\mu}) = [(\bar{\mu} + i\Delta k)^2 + k_p^2]$, and $D_g(\bar{\mu}) = -ik_g^3/\bar{\mu}$. The dispersion relation in the absence of errors is $D(\bar{\mu}_0) = 0$ and is third order in $\bar{\mu}$. In the presence of errors, the right side of (B19) will be nonzero and there will be a shift in wavenumber, $\bar{\mu} \simeq \bar{\mu}_0 + \bar{\mu}_1$ where $\bar{\mu}_0$ is the error-free wavenumber and

$$\bar{\mu}_1 = -\left[\left\langle\delta\mu_n^2\right\rangle + D_g\left\langle\delta\Gamma^2\right\rangle\right]/D'(\bar{\mu}), \tag{B20}$$

with $D'(\bar{\mu}) = dD/d\bar{\mu}$. We may now solve for the constant ρ_0 using the lowest order version of Eq. (B13), $\rho_0 = -D_g^{-1}$.

To evaluate the right side of (B20) we linearize Eqs. (B10) and (B11) for the fluctuating quantities,

$$\delta\mu_+ = -\frac{\delta k^2(z)}{2ik_0} + ik_g^3\rho_0\delta\Gamma, \tag{B21a}$$

and

$$2(\mu_n + i\Delta k)\delta\mu_n + \frac{d}{dz}\delta\mu_n = -\rho_0^{-1}\delta\Gamma, \tag{B21b}$$

which along with (B16) constitute a second order system of linear differential equations for the fluctuating quantities. Using the notation of Eq. (B19) we write this system,

$$\left(\frac{d}{dz} + D'_b\right)\delta\mu_n = D_g\delta\Gamma, \tag{B22a}$$

and

$$\left(\frac{d}{dz} + \bar{\mu}\right)\delta\Gamma = \delta\mu_n + \frac{\delta k^2(z)}{2ik_0}, \tag{B22b}$$

where $D'_b(\bar{\mu}) = dD_b/d\bar{\mu}$. We then write a formal solution to Eqs. (B22) in terms of Green's functions,

$$\delta\Gamma(z) = \int_{-\infty}^{z} dz' G_\Gamma(z-z') \frac{\delta k^2(z')}{2ik_0} \tag{B23a}$$

$$\delta\mu_n(z) = \int_{-\infty}^{z} dz' G_n(z-z') \frac{\delta k^2(z')}{2ik_0}. \tag{B23b}$$

The Green's functions satisfy equations similar to (B22) but with the source replaced by a delta function,

$$\left(\frac{d}{dz} + D_b'\right) G_n = D_g G_\Gamma, \tag{B24a}$$

and

$$\left(\frac{d}{dz} + \bar{\mu}\right) G_\Gamma = G_n + \delta(z). \tag{B24b}$$

The initial conditions for (B24) are that both Green's functions vanish for $z < 0$. Alternatively, we can solve Eqs. (B24) for $z > 0$, without the delta function source, if we take as initial conditions, $G_n(0) = 0$, and $G_\Gamma(0) = 1$. In principle (B24a) and (B24b) can be solved and the solution expressed as a pair of exponentials. We will postpone this step because what will ultimately be needed are integrals of the squares of the Green's functions, and these can be obtained by other means.

Calculation of the growth rate correction due to random errors in (B24) requires evaluation of the square of the fluctuating quantities such as,

$$\left\langle \delta\mu_n^2 \right\rangle = -\frac{\left\langle \left(\delta k^2\right)^2 \right\rangle}{4k_0^2} \int_{-\infty}^{z} dz' G_n(z-z') \times \int_{-\infty}^{z} dz'' G_n(z-z'') C(|z'-z''|). \tag{B25}$$

Here we have assumed that the fluctuations in wavenumber are statistically homogeneous and characterized by a correlation function C, where $\left\langle \delta k^2(z') \delta k^2(z'') \right\rangle = \left\langle (\delta k^2)^2 \right\rangle C(|z'-z''|)$.

We assume that the correlation function is localized to a small range compared with the characteristic growth lengths. A typical correlation length might be one period of a coupled cavity structure. Thus, the integrand in the double integral in (B25) is peaked at $z' = z''$, and can be turned into a single integral of the form,

$$\left\langle \delta\mu_n^2 \right\rangle = -\frac{\left\langle \left(\delta k^2\right)^2 \right\rangle L_c}{4k_0^2} I_{nn}, \tag{B26a}$$

where the correlation length is given by $L_c = \int_{-\infty}^{\infty} dz\, C(|z|)$, and the integral $I_{nn} = \int_0^\infty dz\, G_n^2(z)$. Similar analysis gives

$$\left\langle \delta\Gamma^2 \right\rangle = -\frac{\left\langle \left(\delta k^2\right)^2 \right\rangle L_c}{4k_0^2} I_{\Gamma\Gamma}, \tag{B26b}$$

where the integral $I_{\Gamma\Gamma} = \int_0^\infty dz\, G_\Gamma^2(z)$.

We now turn to the evaluation of the integrals I_{nn} and $I_{\Gamma\Gamma}$. Rather than solve explicitly for the Green's functions and integrate over z, we multiply (B24a) by G_n and (B24b) by G_Γ and integrate from $z = 0^+$ to infinity. We use the initial conditions $G_n(0) = 0$ and $G_\Gamma(0) = 1$, and we assume $G_n, G_\Gamma \to 0$ as $z \to \infty$ to evaluate the end point contributions of the integrals. The result is

$$D_b' I_{nn} = D_g I_{\Gamma n} \tag{B27a}$$

and

$$\bar{\mu} I_{\Gamma\Gamma} - \frac{1}{2} = I_{\Gamma n}, \tag{B27b}$$

where $I_{\Gamma n} = \int_0^\infty dz\, G_\Gamma(z) G_n(z)$. Next, we multiply (B24a) by G_Γ and (B24b) by G_n, integrate from $z = 0^+$ to infinity, and add. This result is

$$\left(D_b' + \bar{\mu}\right) I_{\Gamma n} = D_g I_{\Gamma\Gamma} + I_{nn}. \tag{B27c}$$

Equations (B27) are a linear system that can be solved for the integrals, I_{nn}, $I_{\Gamma n}$, and $I_{\Gamma\Gamma}$. Then we find, after a little algebra

$$\bar{\mu}_1 z = -\frac{\left\langle \left(\delta k^2\right)^2 \right\rangle L_c z}{8k_0^2} \frac{D_b' D_g'}{D'^2}. \tag{B28}$$

Next we wish to cast Eq. (B28) in terms of σ_b. Substituting $q(x) = (v_p(x) - v_{p0})/v_{p0}$ into Eq. (B3) it can be shown that

$$\delta k^2(z) = -2k_0^2 q(x). \tag{B29}$$

The relation $\sigma_b = (\sigma_q/C)(1 + Cb_0)$ allows us to write that

$$\left\langle q^2(x) \right\rangle = \sigma_q^2 = \left[\frac{C\sigma_b}{1+Cb_0}\right]^2. \tag{B30}$$

Taking the derivative of (B19) with respect to $\bar{\mu}$ we define

$$\lambda(\gamma) \equiv \frac{D_b' D_g'}{D'^2} = \frac{2\gamma^2\left(\frac{\Delta k}{k_g} - i\gamma\right)}{\left[1 + 2\gamma^2\left(\frac{\Delta k}{k_g} - i\gamma\right)\right]^2}, \tag{B31}$$

where $\Delta k/k_g = b_0/(1+Cb_0)$ and $\gamma \equiv \bar{\mu}/k_g$. The value of γ is determined by solving the dispersion relationship $D(\bar{\mu}_0) = 0$, which after substituting $k_p^2/k_g^2 = 4QC$ can be written in terms of γ to read

$$\gamma\left[\left(\gamma + \frac{ib_0}{1+Cb_0}\right)^2 + 4QC\right] = i. \tag{B32}$$

Combining Eqs. (B29)–(B31) with (B28) and substituting the correlation length in terms of $x = k_0 z$ as $k_0 L_c = x/N = \Delta$ yields

$$\bar{\mu}_1 z = \langle G_1(x) + j\theta_1(x) \rangle = -\frac{\lambda(\gamma)}{2}\left(\frac{C}{1+Cb_0}\right)^2 \sigma_b^2 x\Delta, \tag{B33}$$

where λ is given by Eq. (B31) and the value of γ is determined by Eq. (B32). Equation (B33) is Eq. (8) of the text. Note that if $b_0 = 0$ and $QC = 0$, then $\Delta k = 0$, $\gamma^3 = i$, and λ is real by Eq. (B31), in which case $\langle\theta_1\rangle = 0$ by Eq. (B33), as in the example in Fig. 2(b).

REFERENCES

[1] J. R. Pierce, *Traveling Wave Tubes*. New York, NY, USA: Van Nostrand, 1950.

[2] A. S. Gilmour, *Microwave Tubes*. Norwood, MA, USA: Artech House, 1986.

[3] V. Granatstein, R. Parker, and C. Armstrong, "Vacuum electronics at the dawn of the twenty-first century," *Proc. IEEE*, vol. 87, no. 5, pp. 702–716, May 1999.

[4] J. H. Booske, D. R. Whaley, W. L. Menninger, R. S. Hollister, and C. M. Armstrong, "Traveling-wave tubes," in *Modern Microwave and Millimeter Wave Power Electronics*. Piscataway, NJ, USA: IEEE Press, 2005, pp. 171–246.

[5] C. Kory and J. Dayton, "Effect of helical slow-wave circuit variations on TWT cold-test characteristics," *IEEE Trans. Electron. Devices*, vol. 45, no. 4, pp. 972–976, Apr. 1998.

[6] N. Luhmann, Jr., G. Caryotakis, G.-S. Park, R. M. Phillips, and G. P. Scheitrum, "Affordable manufacturing," in *Modern Microwave and Millimeter Wave Power Electronics*. Piscataway, NJ, USA: IEEE Press, 2005, pp. 731–763.

[7] P. Pengvanich, D. Chernin, Y. Y. Lau, J. W. Luginsland, and R. M. Gilgenbach, "Effect of random circuit fabrication errors on small-signal gain and phase in traveling-wave tubes," *IEEE Trans. Electron Devices*, vol. 55, no. 3, pp. 916–924, Mar. 2008.

[8] D. Chernin, I. Rittersdorf, Y. Y. Lau, T. M. Antonsen, and B. Levush, "Effects of multiple internal reflections on the small-signal gain and phase of a TWT," *IEEE Trans. Electron Devices*, vol. 59, no. 5, pp. 1542–1550, May 2012.

[9] H. R. Johnson, "Backward-wave oscillators," *Proc. IRE*, vol. 43, no. 6, pp. 684–697, 1955.

[10] S. Sengele, M. L. Barsanti, T. A. Hargrave, C. M. Armstrong, J. H. Booske, and Y. Y. Lau, "Impact on random manufacturing errors on backwave-wave small-signal gain in traveling wave tubes with finite space charge electron beams," *J. Appl. Phys.*, vol. 113, no. 7, pp. 074905-1–074905-9, 2013.

Ian M. Rittersdorf (S'11) received the B.S.E. and M.S.E. degrees in nuclear engineering and radiological sciences from the University of Michigan, Ann Arbor, MI, USA, in 2008 and 2010, respectively, where he is currently pursuing the Ph.D. degree.

His current research interests include general theory of oscillators, theory of magneto-Rayleigh-Taylor instability, and tube-based microwave sources.

Mr. Rittersdorf is a student member of the American Physical Society. He was a recipient of the Michigan Institute for Plasma Science and Engineering Fellowship in 2011.

Thomas M. Antonsen, Jr. (F'11) was born in Hackensack, NJ, USA, in 1950. He received the B.S. degree in electrical engineering and the M.S. and Ph.D. degrees from Cornell University, Ithaca, NY, USA, in 1973, 1976, and 1977, respectively.

From 1976 to 1977, he was a National Research Council Post-Doctoral Fellow with the Naval Research Laboratory, Washington, DC, USA. From 1977 to 1980, he was a Research Scientist with the Research Laboratory of Electronics, Massachusetts Institute of Technology (MIT), Cambridge, MA, USA. In 1980, he was with the University of Maryland, College Park, MD, USA, where he joined the faculty of the Department of Electrical Engineering and the Department of Physics in 1984, was the Acting Director of the Institute for Plasma Research, University of Maryland from 1998 to 2000, and is currently a Professor of Physics and Electrical and Computer Engineering. He has held visiting appointments with the Kavli Institute for Theoretical Physics, University of California, Santa Barbara, CA, USA, the Ecole Polytechnique Fédérale de Lausanne, Lausanne, Switzerland, and the Centre de Physique Théorique, Ecole Polytechnique, Palaiseau, France. He is the author or a co-author of more than 300 journal articles and a co-author of the book, *Principles of Free-Electron Lasers*. His current research interests include the theory of magnetically confined plasmas, the theory and design of high-power sources of coherent radiation, nonlinear dynamics in fluids, and the theory of the interaction of intense laser pulses and plasmas. Dr. Antonsen was a fellow in 1986 of the Division of Plasma Physics, American Physical Society, for which he served as the Chair in 2010. He has served on the Editorial Board of *Physical Review Letters*, *The Physics of Fluids*, and *Comments on Plasma Physics*. He was a co-recipient of the 1999 Robert L. Woods Award for Excellence in Vacuum Electronics Technology and was the recipient of the IEEE Plasma Science and Applications Award in 2003 and the Outstanding Faculty Research Award from the Clark School of Engineering in 2004.

David Chernin received the B.A. and Ph.D. degrees in applied mathematics from Harvard University, Cambridge, MA, USA, in 1971 and 1976, respectively. From 1976 to 1978, he was a member of the Institute for Advanced Study, Princeton, NJ, USA, where he focused on problems in magnetic confinement fusion. From 1978 to 1981, he was a Senior Scientist with Maxwell Laboratories, San Diego, CA, USA, where he focused on the design and analysis of excimer lasers and high-power X-ray sources. Since 1984, he has been with Science Applications International Corporation (SAIC), McLean, VA, USA, where he has conducted research on the theory and simulation of beam-wave interactions in particle accelerators and on the design, simulation, and analysis of vacuum electron devices in collaboration with the Vacuum Electronics Branch, Naval Research Laboratory, Washington, DC, USA. From 2005 to 2008, he served as the Chief Scientist with the Technology and Advanced Systems Business Unit, SAIC.

Dr. Chernin is a member of the American Physical Society.

Y. Y. Lau (M'98–SM'06–F'08) received the B.S., M.S., and Ph.D. degrees in electrical engineering from the Massachusetts Institute of Technology (MIT), Cambridge, MA, USA, in 1968, 1970, and 1973, respectively.

From 1973 to 1979, he was an Instructor and an Assistant Professor of applied mathematics with MIT. From 1980 to 1983, he was with Science Applications International Corporation, McLean, VA, USA, as a Research Physicist. From 1983 to 1992, he was a Research Physicist with the Naval Research Laboratory, Washington, DC, USA. In 1992, he joined the University of Michigan, Ann Arbor, MI, USA, where he is currently a Professor with the Department of Nuclear Engineering and Radiological Sciences and the Applied Physics Program. He is a Faculty Appointee at the Naval Research Laboratory. He has been involved in electron beams, coherent radiation sources, plasmas, and discharges. He is the author or a co-author of more than 190 refereed publications. He holds ten patents. His current research interests include electrical contacts, heating phenomenology, high-power microwave sources, and magneto-Rayleigh-Taylor instabilities.

Dr. Lau is a fellow of the American Physical Society. He received the 1989 Sigma-Xi Scientific Society Applied Science Award and the 1999 IEEE Plasma Science and Applications Award. He served three terms from 1994 to 2005 as an Associate Editor for *Physics of Plasmas*.